# Chapter 22

# Application of Roving Mass Technique Associated with Wavelet Transform to Structural Damage Detection and Localization

### Chapter details

**Chapter DOI:**

https://doi.org/10.4322/978-65-86503-83-8.c22

**Chapter suggested citation / reference style:**

Palechor, Erwin U. L., et al. (2022). “Application of Roving Mass Technique Associated with Wavelet Transform to Structural Damage Detection and Localization”. *In* Jorge, Ariosto B., et al. (Eds.) *Fundamental Concepts and Models for the Direct Problem*, Vol. II, UnB, Brasilia, DF, Brazil, pp. 881–898. Book series in Discrete Models, Inverse Methods, & Uncertainty Modeling in Structural Integrity.

**P.S.:** DOI may be included at the end of citation, for completeness.

### Book details

**Book:** Fundamental Concepts and Models for the Direct Problem

**Edited by:** Jorge, Ariosto B., Anflor, Carla T. M., Gomes, Guilherme F., & Carneiro, Sergio H. S.

**Volume II of Book Series in:**

Discrete Models, Inverse Methods, & Uncertainty Modeling in Structural Integrity

**Published by:** UnB City: Brasilia, DF, Brazil Year: 2022

**DOI:** https://doi.org/10.4322/978-65-86503-83-8

# Application of Roving Mass Technique Associated with Wavelet Transform to Structural Damage Detection and Localization

Erwin Ulises Lopez Palechor[1], Juliana C. Santos[2], Ramon Saleno, Yure Costa Silva[3], Marcela R. Machado[2,3], Marcus V. Girão de Morais[2,3*], Luciano Mendes Bezerra[4] and Ariosto Bretanha Jorge[2]

[1] Science and Technology Center, Federal University of Cariri, Brazil. e-mail: erwin.lopez@ufca.edu.br
[2]Post-Graduate Program in Integrity of Engineering Materials, University of Brasilia, Brazil. e-mail: ariosto.b.jorge@gmail.com
[3] Faculty of Technology, University of Brasilia, Brazil. e-mail: ggomes@unb.br; ramon.silva@unb.br; mvmorais@unb.br
[4] Post-Graduate Program in Structures and Civil Construction, University of Brasilia, Brazil. e-mail: lmbz@unb.br

*Corresponding author

***Abstract***

*This chapter presents applications of the roving mass technique associated to Wavelet transforms in damage identification and localization, in beam-like structures, using numerical and experimental data, the research works developed at the Graduate Programs of Integrity of Engineering Materials and Structures and Civil Construction of University of Brasília.*

**Keywords**: Wavelet application, Structural Health Monitoring, Wavelet Transform, Continuous Wavelet, Discrete Wavelet, Wavelet Family Function.

## 1 Introduction

Structural pathologies or even structural collapse are often initiated by cracks in structural members. Structural damages must be identified in its initial state before compromising the integrity and service life of the structure. However, in its initial state, a crack is relatively small making it difficult to detect changes in the dynamic properties. Moreover, there are situations where damages may be hidden due to external cover façade, finishing, or skinning of buildings, bridges, etc. turning the detection of damages a difficult process. Therefore, auxiliary tools to indicate possible existence of damages are always welcome.

Aktan et all (1997) introduced the firsts concepts of structural identification. However, methods for identifying cracks, based on the changes of dynamic properties of bridges and buildings, are not very well effective and practical. Moreover, depending on the size of the surface crack, a crack can be detected using traditional technique like the visual inspection. However, it is not possible to visually identify cracks when the structure surface is covered, insulated or located in unreachable locations. To overcome these difficulties, numerical/computational techniques have been under development (Breysse *et al.*, 2008; Schabowicz, 2010) thus enabling quick decision-making process concerning the minimization or elimination of damages.

From the point of view of safety and economy, the detection of damages especially in bridges is an important issue. It is essential to perform periodic inspection to detect changes in the structural stability (Radzieński, Krawczuk and Palacz, 2011). Recent research on the technical literature shows that many damage identification algorithms were developed using dynamic characteristics, especially in the frequency domain (Doebling *et al.*, 1996). In general, these techniques use comparisons between the intact and damaged response of the structure. Techniques based on Wavelet Transforms can overcome this limitation. Such techniques have been applied over the years and have been presented satisfactory results (Wang and Deng, 1999; Law *et al.*, 2005; Ren and Sun, 2008; Liu, Li and Zhang, 2009; Mikami, Beskhyroun and Oshima, 2009; Palechor *et al.*, 2014).

The purpose of this report is presents applications of the roving mass technique associated to Wavelet transforms in damage identification and localization, in beam-like structures, using numerical and experimental data. The research works was developed at the Graduate Programs of Integrity of Engineering Materials and Structures and Civil Construction of University of Brasilia. The numerical analysis models damage beams by Timoshenko FE model with additional mass. And the experimental essay applies non-stationary forces signal to excite commercial profiles of steel beams simply supported (close to real situations).

Firstly, Section 2 presents a description of the roving mass technique and a dimensional analysis of principal parameters. Section 3 carries out a numerical analysis using Timoshenko FE model combined with wavelet transform. Finally, section 4 presents experimental results of a steel beam obtained in Vibration Laboratory of Dynamical Systems Group developed by Graduate Programs of Structures and Civil Construction and Integrity of Engineering Materials of University of Brasília.

## 2 Roving Masses Technique

Damage identification may be seen as an inverse problem of identification of a system whose input signals and output signals are known, but the geometry of the damage location and shape are unknown (Ticona Melo *et al.*, 2016). This means that the purpose of damage detection is to describe a damage in an existing structural model, based on output data obtained experimentally (dynamic response) from specific input signals. It is often desirable to detect irregularities or changes in structure response, considering properties that have been altered by the presence of the damage in the structure.

Studies of identification of damage in structures using an auxiliary mass have been done (Mermetas and Erol, 2001; Zhong and Oyadiji, 2008; Zhong, Oyadiji and Ding, 2008; Erwin Ulises Lopez Palechor *et al.*, 2018; Palechor, Bezerra, Morais, *et al.*, 2019; Santos *et al.*, 2019). This technique consists of the application of an additional mass along the length of structure to magnify the effect of the discontinuities.

In free vibration case, the Euler-Bernoulli beam's motion equation beams is described by follow expression,

$$EI\frac{\partial^4 u}{\partial x^4} + [\rho A + m_a \delta(x - L_d)]\frac{\partial^2 u}{\partial t^2} = 0, \tag{1}$$

where $E$ and $\rho$ are Young modulus and density, respectively, cross-sectional area $A$, beam length $L$, $u$ is the transverse displacements (and acceleration $\ddot{u}$), and $m_d$ is the damage mass.

To obtain the dimensionless of Euler-Bernoulli beam equation, we assume $u = \delta_u \bar{u}$, (beam static deflection $\delta_u$), $x = L\bar{x}$ and $t = T\bar{t} = \bar{t}/f_n$ ($f_n = 1/T$ is the fundamental frequency) in which $\bar{u}$, $\bar{x}$, and $\bar{t}$ are dimensionless parameters.

$$\frac{4\pi^2}{\beta^4}\bar{u}^{IV} + \ddot{\bar{u}} + \frac{m_d}{\rho AL}\ddot{\bar{u}}\delta\left(\bar{x} - \frac{L_d}{L}\right) = 0, \tag{2}$$

where, the dynamic characteristic of beam is described by the parameters $\beta$ (done by expression $2\pi f_n = (\beta^2/L^2)\sqrt{EI/\rho A}$) and function of boundary conditions), mass discontinuity $m_d$ and its position $L_d$. For the present analysis, the damage beam is characterized by the presence of mass discontinuity to simulate an open crack, i.e., a rigidity discontinuity. Santos (2019; 2020) shows the correspondence between mass and rigidity discontinuity for small values.

Frequency-shift curve is the modal frequency of damage beam (with mass discontinuity for this analysis) as function of a roving mass along essayed beam. Zhong Oyadiji (2008) and Zhong Oyadiji and Ding (2008) shows the possibility to determine damage location in beam-like structures by discontinuity in curvature of frequency-shift for first frequencies. Palechor et al. (2014; 2018; 2019) use Discrete Wavelet Transform (DWT) to evidence discontinuity in frequency-shift curves with good results.

## 3 Numerical Damage Identification in Beam-like Structures with Roving Masses Technique

This work section presented a numerical study of additional mass spatial probing identification technique using DWT of frequency shift curves of damaged Timoshenko FE 2-nodes beam (Santos *et al.*, 2019; Santos, 2020). Simply supported and free-free beams was analyzed for two damage mass, ¼ and ½ of beam span. WDR index is proposed to analyze the magnitude of the damage.

Numerical analyses of an aluminum beam with geometric and material properties are presented in Table 1.

**Table 1: Geometric and material properties of the aluminum beam.**

| Characteristics of the beam | |
|---|---|
| Mass [g] | 385,33 |
| Length [m] | 395,00 |
| Base of the cross-section [m] | 19,00 |
| Height of the cross-section [m] | 19,00 |
| Cross section area [mm²] | 361,00 |
| Moment of inertia [mm⁴] | $1{,}09.10^{-4}$ |
| Modulus of elasticity [GPa] | 66,66 |
| Shear modulus [GPa] | 24,18 |
| Density [kg/m³] | 2702,27 |
| Poisson's ratio | 0,33 |

Free-Free (F-F) and Supported-Supported (S-S) boundary conditions are studied. The damage was simulated as discontinuity mass positioned at half and a quarter span from left support, respectively, L/2 and L/4 (Figure 1).

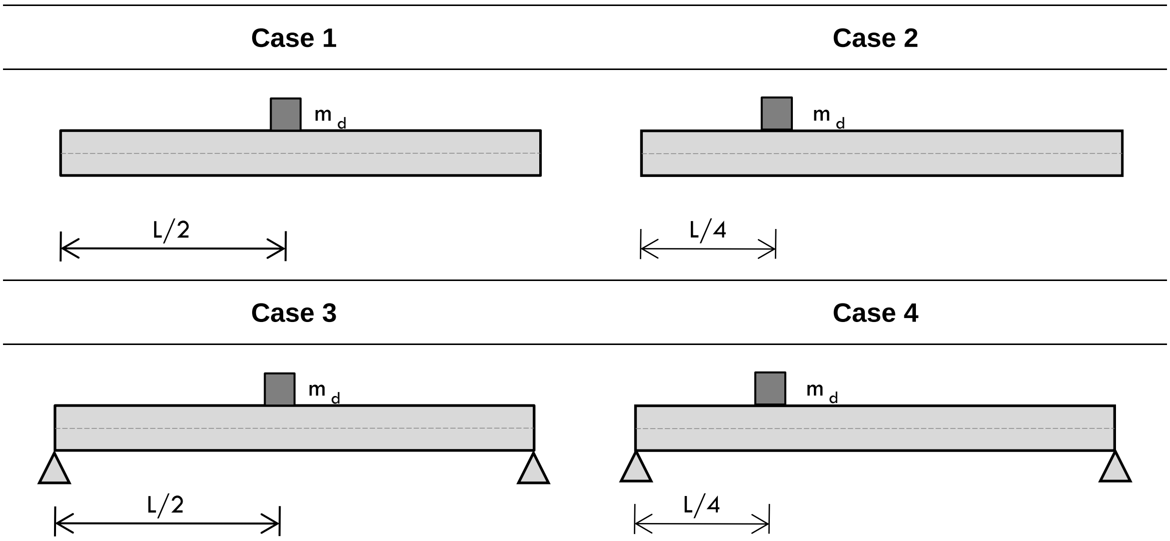


**Figure 1: Beam cases with different boundary conditions and damage positions.**

## 3.1 Frequency-Shift Curve

The frequency-shift technique was applied for three first modal frequencies for each case. Using a roving mass $m_a$ of 2% of total beam mass $m_t$, the frequency-shift curve was used to determine a discontinuity mass $m_d$ varied from 1% to 10% of $m_t$. Figure 2 and Figure 3 shows the frequency-shift curves for F-F and S-S beams, respectively, as function of discontinuity mass $m_d$. It was observed the influence of the structure's mode shape. But, also, it was observed minor variations in frequency-shift curve when discontinuity mass is located at a nodal point (Figure 2b1, Figure 2a2 nd Figure 3b1).

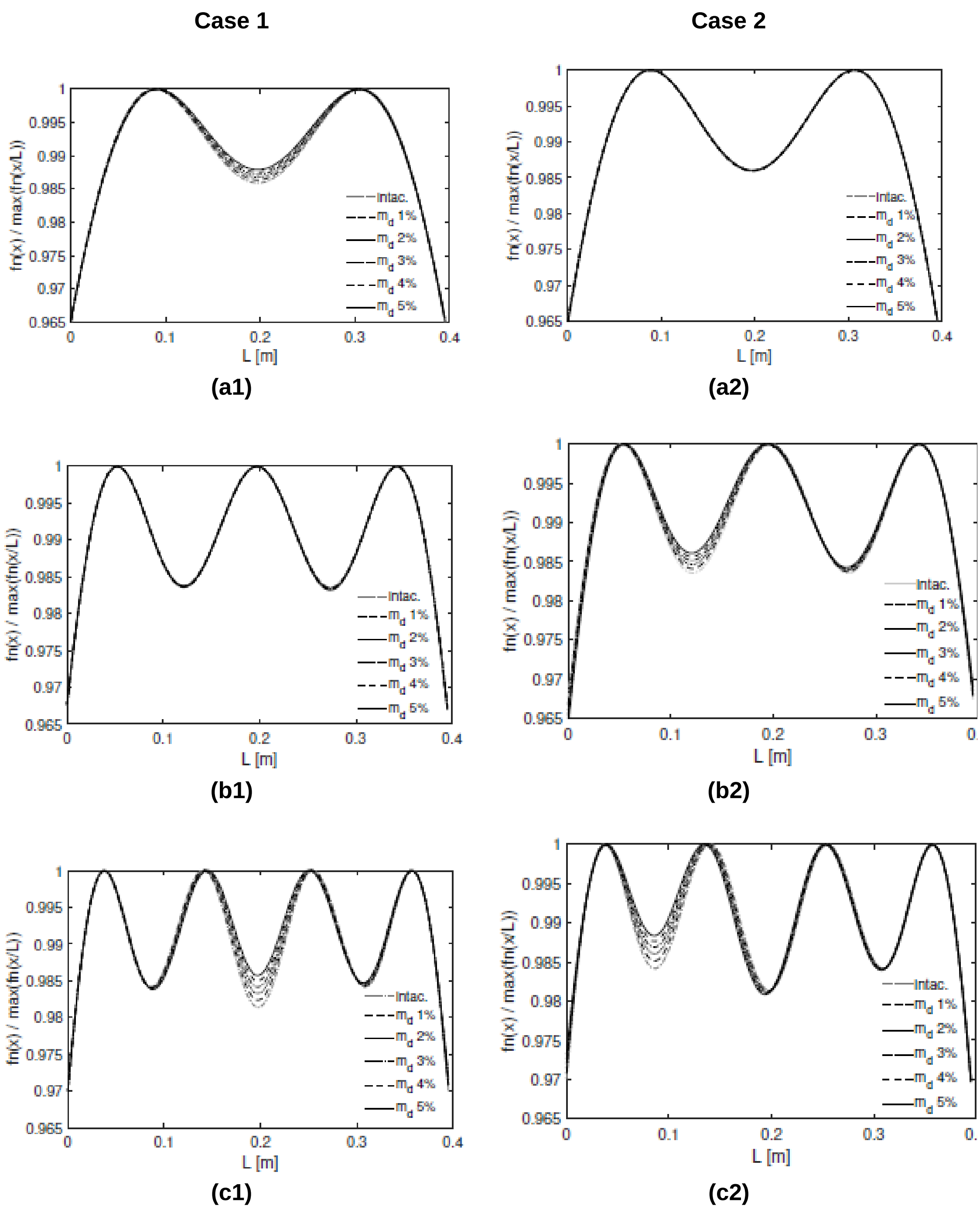


**Figure 2: Frequency-shift $f_n(x/L)/max\ (f_n(x/L))$ function of $m_a$ position in F-F beams (cases C1 and C)2: (a) first frequency, (b) second frequency and (c) third frequency.**

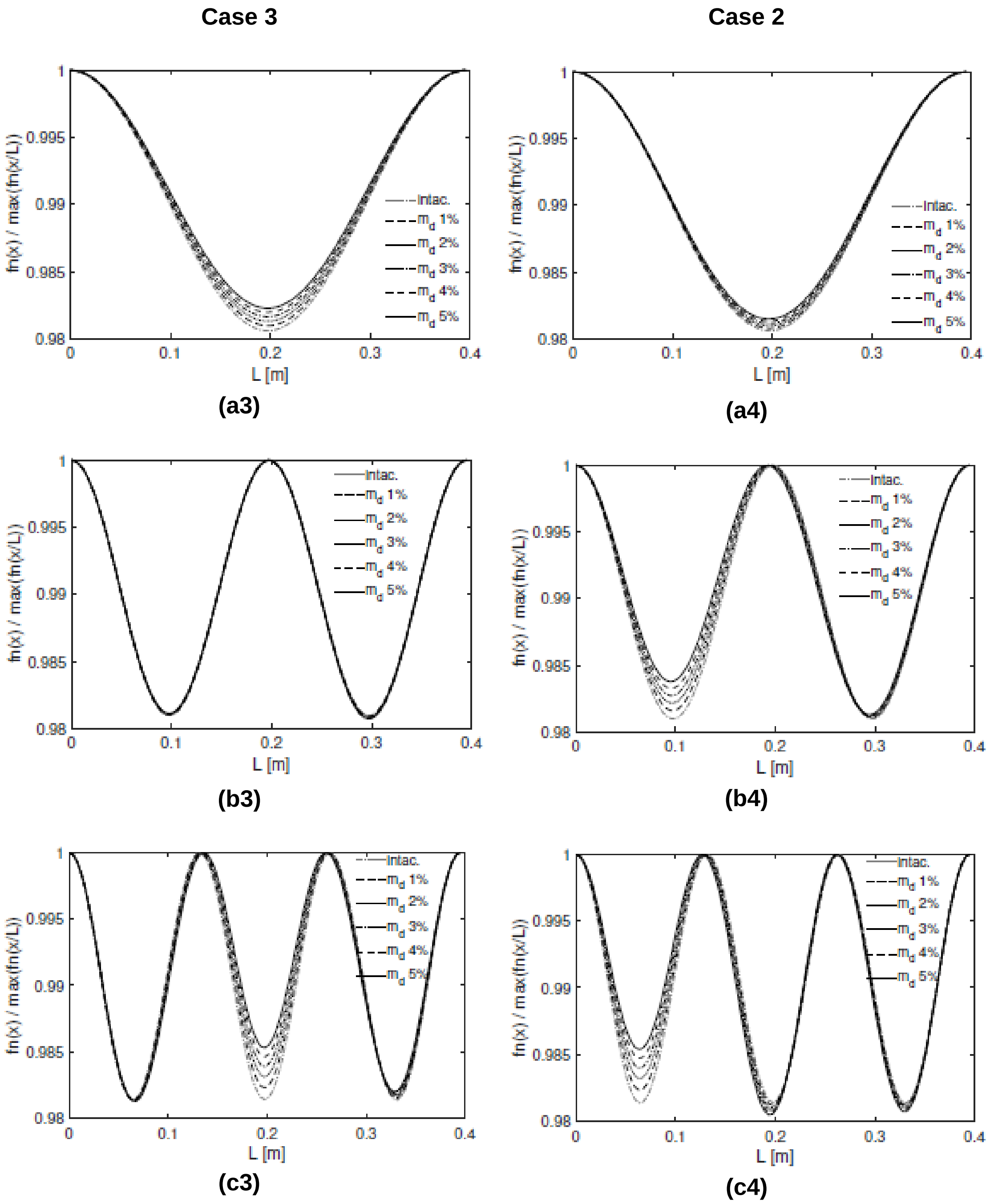


**Figure 3: Frequency-shift $f_n(x/L)/max(f_n(x/L))$ function of $m_a$ position in S-S beams (cases C1 and C)2: (a) first frequency, (b) second frequency and (c) third frequency.**

### 3.2 DWT of roving mass ($m_a$) and damage mass ($m_d$) relationship

For a discontinuity mass located at middle span of F-F (C1) and S-S (C3) beams, using the bior6.8 mother wavelet, the influence of the additional mass $m_a$ on the frequency shift curve is studied. To define a useful metric, it is proposed wavelet damage ratio (WDR) that relate damage level by the ratio between damage signal $S_d$ and base signal $S_b$ (Figure 4).

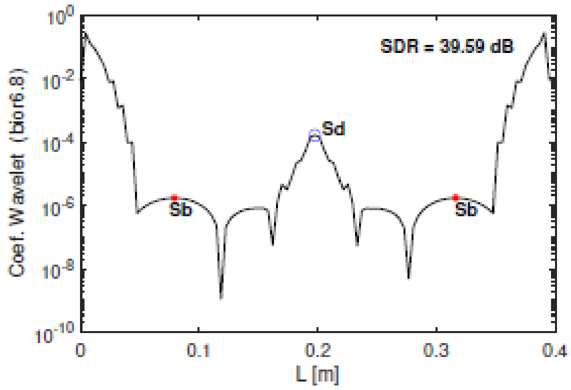


**Figure 4: WDR index determination using the wavelet functions bior6.8.**

The WDR index is expressed by equation,

$$WDR[dB] = 20log_{10}\left(\frac{Sd}{Sb}\right), \tag{3}$$

in which $S_d$ and $S_b$ corresponds, respectively, to the maximum absolute value of DWT coefficient at damage position and without singularities positions, as shown in Figure 4. Figure and Figure 6 present frequency-shift curve for 1 and 10% damage relative to roving masses of 1, 2 and 5% additional mass.

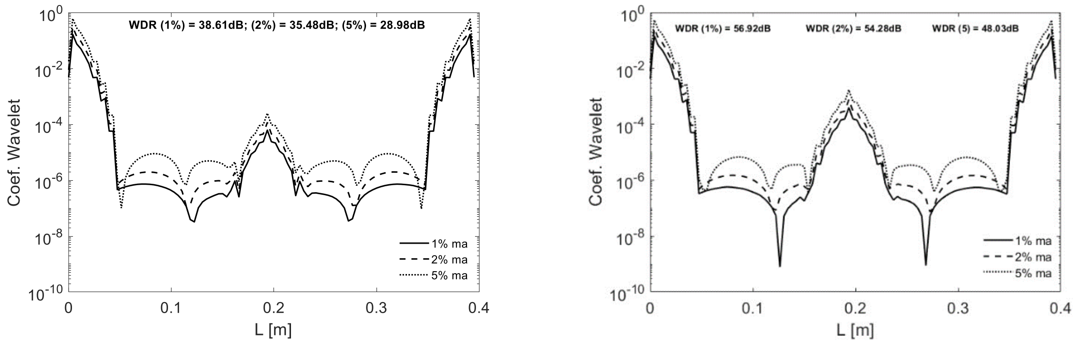


(a) (b)

**Figure 5: Frequency-shift curve of C1 beam as function of roving mass $m_a$ for damage mass $m_d$ of 1% (a) and 10% (b).**

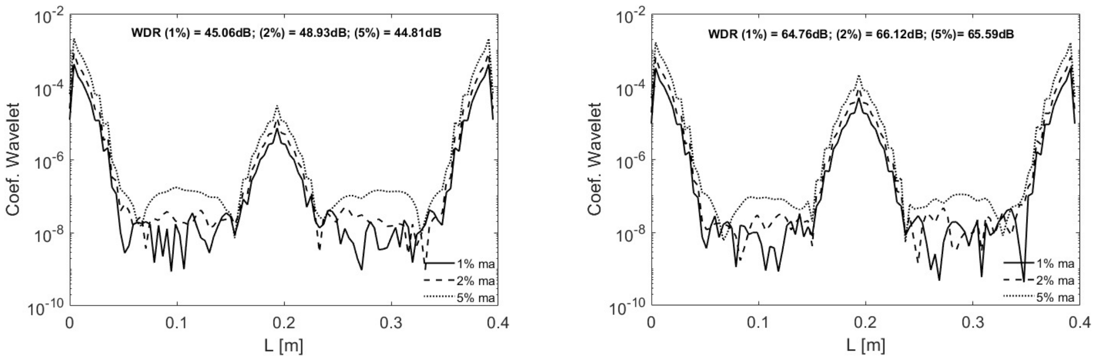


(a) (b)

**Figure 6: Frequency-shift curve of C1 beam as function of roving mass $m_a$ for damage mass $m_d$ of 1% (a) and 10% (b).**

Figure  show WDR index for additional mass of 5% with a slight tendency to saturation. Figure 6 present the same tendency in this regard. Increasing of roving mass does not improve the damage perception, i.e., an increase in WDR.

### 3.3 Final Comments on the Numerical Example

The frequency-shift curve makes possible detect and locate a damage using only damaged response, eliminating comparison to an intact response. The proposition of WDR index as a metric to reduce frequency-shift curve to a value need more analysis. The damage perception was not increased with more roving mass. Palechor (2013) have the same impression in his experimental study. But it is necessary more numerical and experimental observation about this question.

## 4 Experimental Damage Identification in Beam-like Structures with Roving Masses Technique

This work presents the application of an identification methodology based on the analysis of the dynamic properties of simply supported steel beams. Beams here are submitted to the action of additional masses that can generate progressive changes of the natural frequencies (Mermetas and Erol, 2001; E. U.L. Palechor *et al.*, 2018). The change in the structural stiffness due to the existence of damage in the beam may not be so evident. Therefore, in this research, the Wavelet Transform is used to help in the process of locating possible stiffness changes due to damages (Rizos, Aspragathos and Dimarogonas, 1990; Mermetas and Erol, 2001; Kotambkar, 2014; Khoa and Quang, 2016). This research also presents experimental tests results on steel beams with simulated damages. The experimental tests were carried out in the Laboratory of Vibrations of the Department of Mechanical Engineering in the University of Brasília. Even though the experiments were conducted within the laboratory, the size of the beams tested corresponds to small commercialized steel beams available in the market.

The additional mass placed on the beams were small steel plates fixed with braces and bolts. The assembly of the added masses is schematically shown in Figure 7.

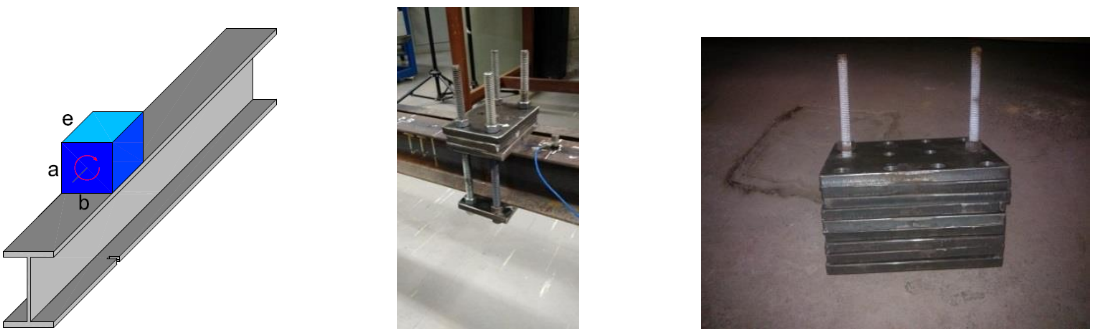


**(a) Additional Mass** **(b) Additional Mass** **(c) Steel plate to add mass.**

**Figure 7: Additional mass on the beam.**

Figure 8 show schematic representation for location and characteristics of induced damage on essayed beams. The additional masses (M) add together 3.366 kg for Case C1 and 24.718 kg for Case C2.

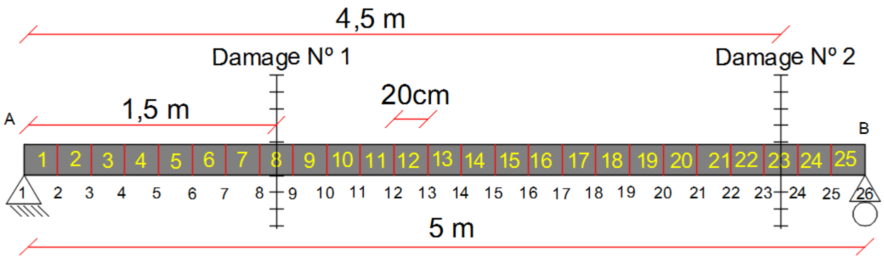


**(a) Case C1**

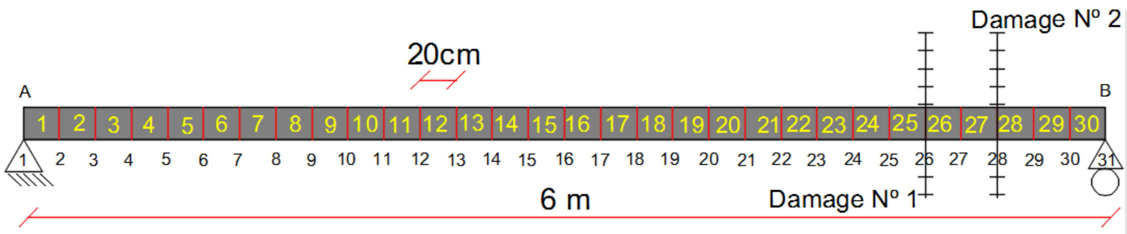


**(b) Case C2**

**Figure 8: Schematic representation of Damage Position for Cases 1 (a) and 2 (b)**

Figure 9 shows details of the test scheme assemblage the steel beams in the Laboratory of Vibration and Dynamics of Systems of the University of Brasília.

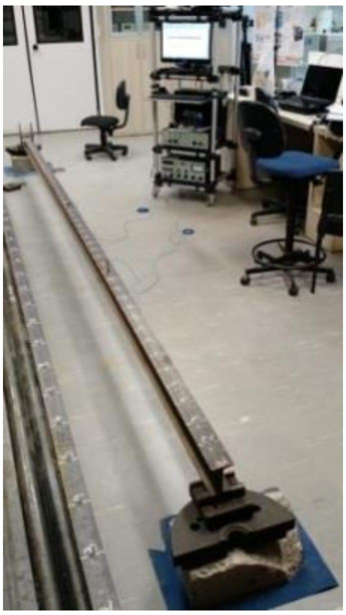
(a)

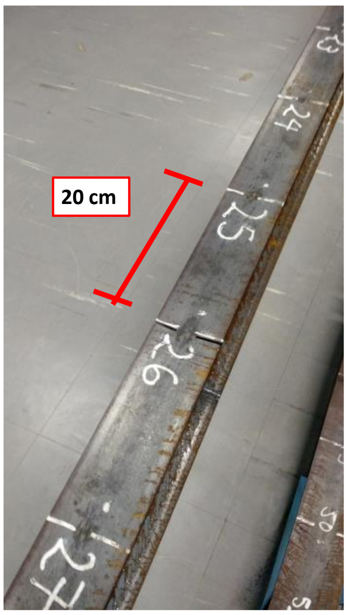

(b)

**Figure 9: Experimental setup of simply support beam: (a) general view of essayed beam, and (b) detail of measurement points (discretization of 20cm).**

To ensure simple support (Figure 10a), two plane plates and a roller were used to allow displacement only in the x direction. For the hinged support (Figure 10b), two grooved plates with a roller were designed to restrict the translation in all direction, permitting only rotation.

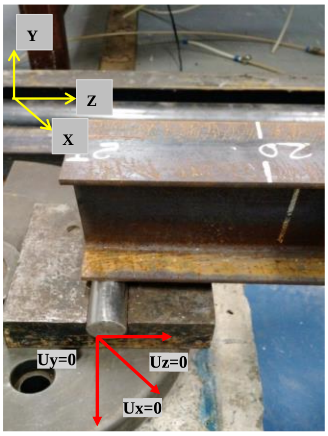


(a) Left Support.

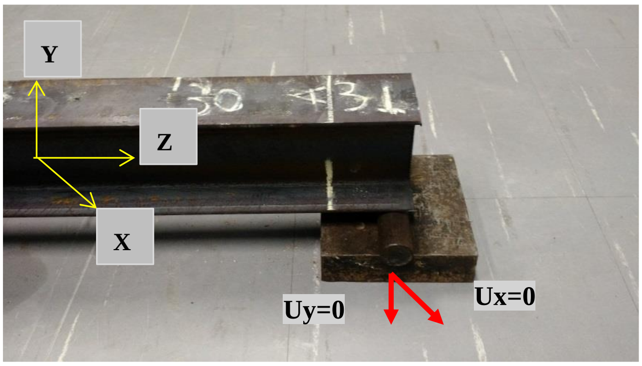


(b) Right support.

**Figure 10: Detail for simple support at steel beam ends.**

In order to carry out the dynamic tests the following tools are used accelerometers PCB 352C34 and PCB352C33, modal hammer PCB 086C0 (with steel tip) and NI cDAQ + NI 9187 + LabView software as data acquisition.

The experimental procedure follows the steps below for each roving mass position:

- **Step 1**: the experimental specimens were subjected to impact load (modal hammer) applied in middle span (Figure 11).

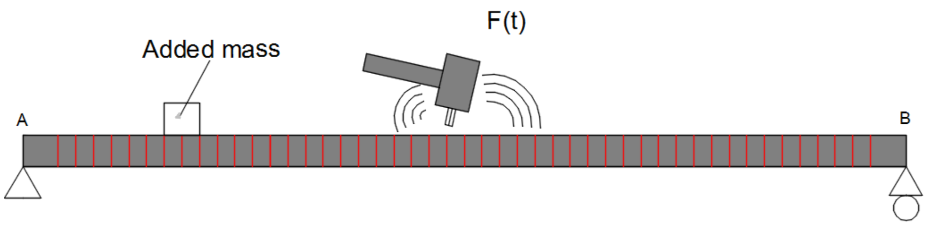


**Figure 11: Impact modal analysis for beam essayed with roving mass.**

- **Step 2**: Force and acceleration dynamic signals was acquired by NI+Labview signal conditioner (Figure 12). This modal impact test was carried out four times. Exponential ad force windows were applied to acceleration and force signal, respectively, to reduce leakage effect. Force and acceleration temporal signals were saved for posterior treatment.
- **Step 3**: Estimation of inertance response of force and acceleration dynamic signals by a Matlab script. First modal frequencies were accurately identified performing a weighted average of values around a peak detected in spectrum response.

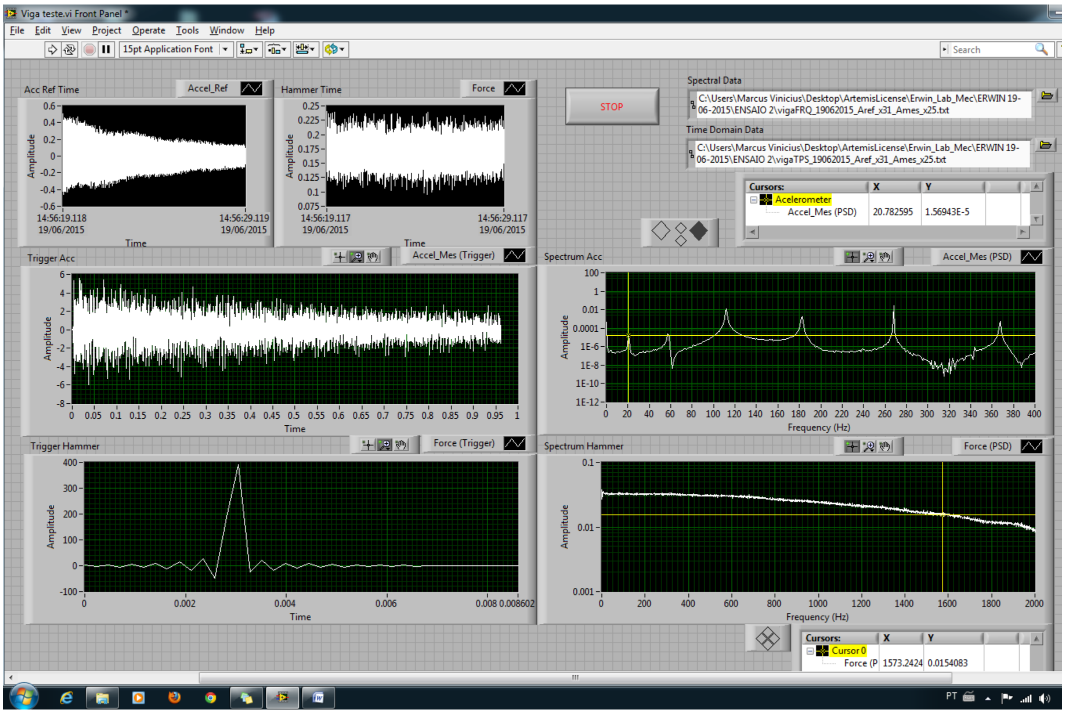


**Figure 12: LabView control panel.**

The frequency resolution is very important to determine frequency variations due to additional mass location along essayed beam. Thus, several parameters are necessary configure to be able the analysis of dynamic signals: analyzed data size (N), acquisition rate (Δt) and sampling frequency (Fs). The best results were obtained with the following parameters: (a) $Fs = 1653\,Hz$, (b) $\Delta t\ = 0.000605\,s$, and (c) $N = 16384\,(2^{14})$.

Once inertance FRF estimated (Figure 13), the peaks correspond to firsts modal frequencies are identified for each roving mass position. After the peak identification, the estimated modal frequency $f_{n,est}$ is performed a weighted average of frequencies around the lobe of spectrum frequency (National Instruments, 2009).

$$f_{n,est} = \frac{\sum_{i=j-m}^{j+m} Power(i)\ i\ \Delta f}{\sum_{i=j-m}^{j+m} Power(i)} \tag{4}$$

where, $j$ is array position of frequency peak and $Power\ (i)$ represents the amplitude value of FRF spectral line.

Once the corrected frequencies are obtained, these values are plotted to compound the frequency-shift curve. The discretization of essayed beam for roving mass position was done by 20 cm. For C1 and C2 beams (5m and 6m long), respectively, there are 26 and 31 positions for the roving mass. The frequency-shift curve are interpolated to obtain a vector with a larger number of data and thus calculate the wavelet coefficients as described in Palechor *et al.* (Palechor, 2013; Palechor, Bezerra, Morais, *et al.*, 2019; Palechor *et al.*, 2022).

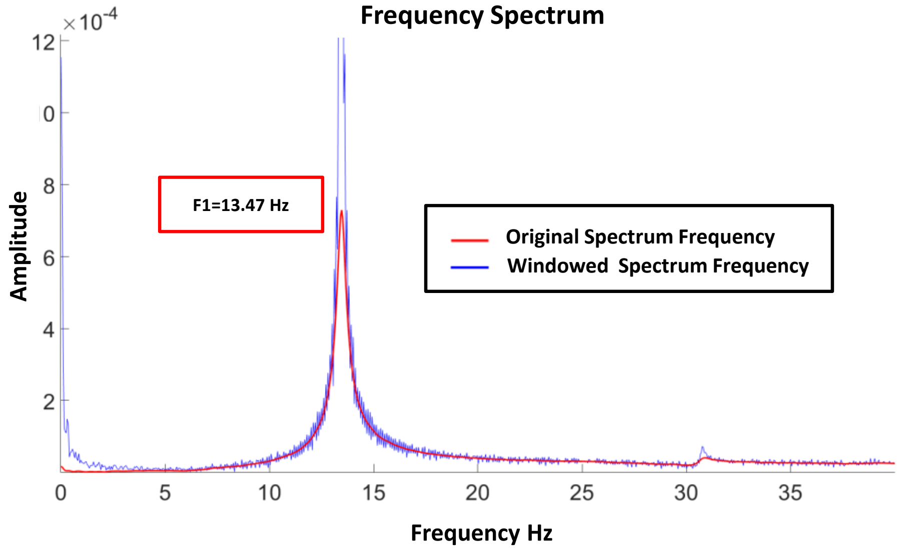


**Figure 13: Example of inertance FRF spectrum for essayed beam with a roving mass.**

In the frequency domain, the peaks corresponding to the first natural frequency of the structure are identified. Figure 13 shows an example inertance FRF spectrum with/without application of the exponential window. Noise reduction and signal stabilization are clearly visible due to the use of the exponential window.

## 4.1 Experimental Results of Case C1

Figure 14 represents the frequency-shift curve for first frequency of case C1 beam. This graph corresponds to first frequency of C1 beam as function of roving mass position along its 26 measured nodes. The added mass used was 3.266 kg, positioned on each node.

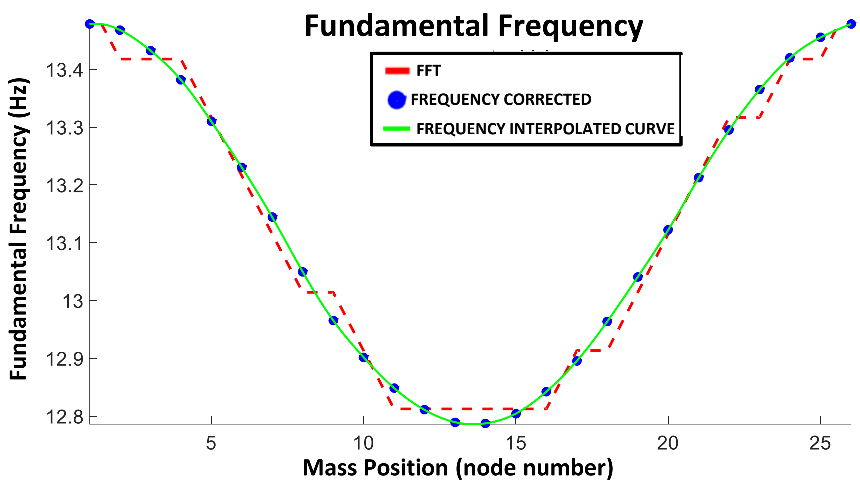


**Figure 14: Frequency-shift curve for first frequency of beam C1.**

In Figure 14, the dashed line represents the FRF peak frequencies. The dotted line is estimated frequency using Equation (4). And the solid line is the cubic spline interpolation of estimated frequency (Erwin Ulises Lopez Palechor *et al.*, 2018; Palechor, Bezerra, Morais, *et al.*, 2019; Palechor *et al.*, 2022). This numerical interpolation obtains best fits signals to damage location.

Figure 15 are the DWT of frequency-shift curve using four mother wavelet functions (sym6, rbio2.6, db5 and bior6.8). It can be observed a group of spikes between nodes 8 and 9 and between nodes 23 and 24 which matches to damage located at 1.5m and 4.5m, respectively. This last one shows less prominent, but still noticeable. Such peaks are big enough to be seen compared with the other peaks exists.

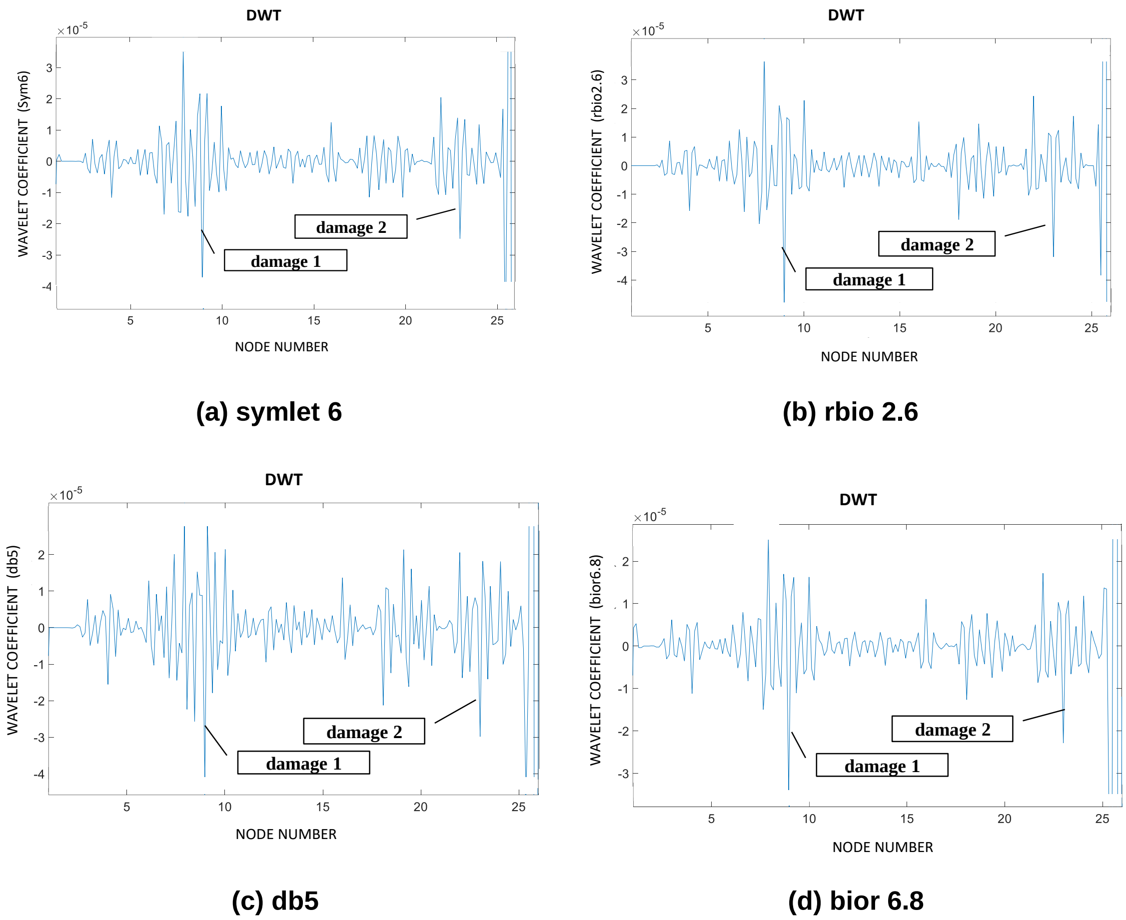


**(a) symlet 6** **(b) rbio 2.6**

**(c) db5** **(d) bior 6.8**

**Figure 15: DWT first frequency using (a) symlet 6, (b) rbio2.6, (c) db5 and (d) bior 6.8 mother wavelets.**

## 4.2 Experimental Results of Case C2

Figure 16 represents frequency-shift curve for first frequency of case C2 beam. This graph corresponds to first frequency of C2 beam as function of roving mass position along its 31 measured nodes. The roving mass used was 24.718 kg, positioned on each node.

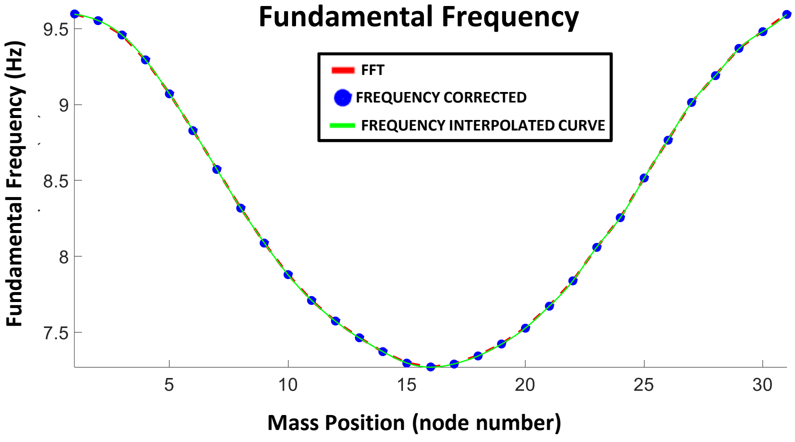


**Figure 16: Frequency-shift curve for first frequency of beam C2.**

Figure 17 presents the DWT of frequency-shift curve using four mother wavelet functions (sym6, rbio2.6, db5 and bior6.8). It can be observed a group of spikes between nodes 25 and 27 and between nodes 28 and 29 which matches to damages induced. The techniques of signal interpolation with the cubic spline in the frequency domain and the method of main lobe correction showed good results.

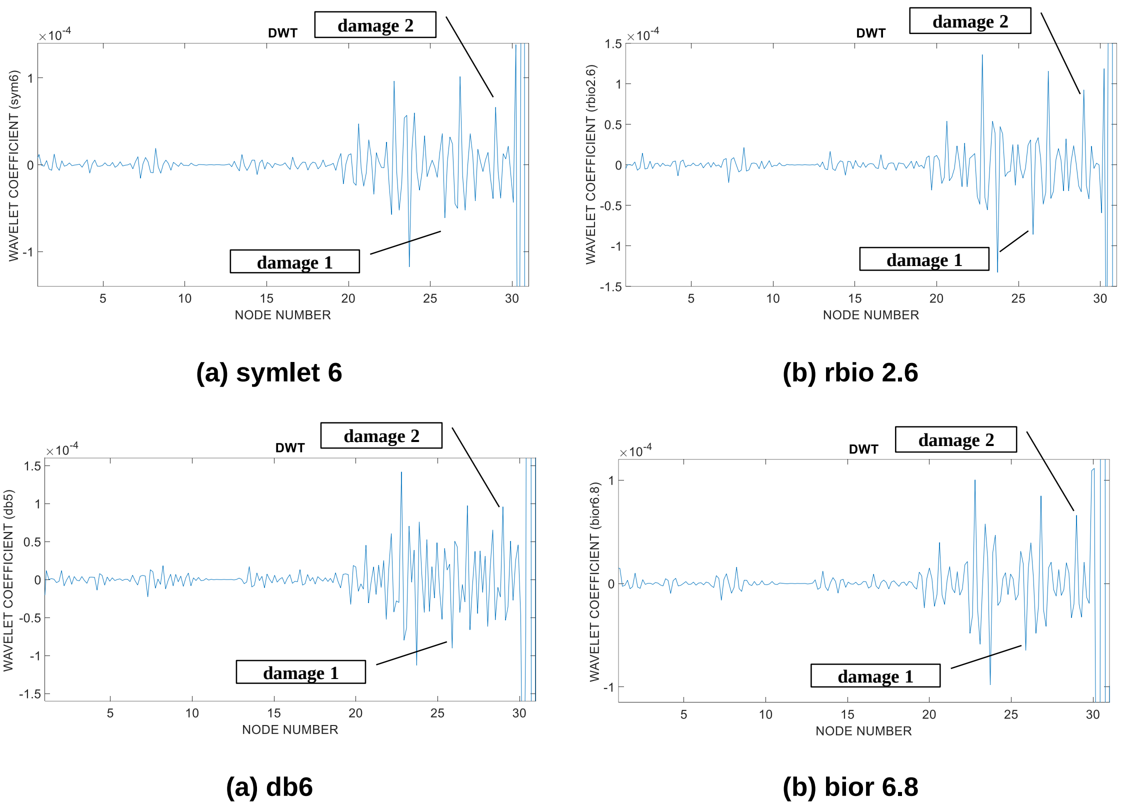


**Figure 17: DWT first frequency using (a) symlet 6, (b) rbio2.6, (c) db5 and (d) bior 6.8 mother wavelets.**

### 4.3 Final Comments on the Experimental Example

This section presented experimental results using roving mass technique to locate damages in essayed beams with simulated open cracks. Measuring of fundamental frequency of essayed beams with an added mass positioned along it. Two cases were analyzed: case C1 and C2, respectively, with 5m and 6m. Both beams are commercial steel I-section. The damage is responsible for pronounced peaks clusters on DWT coefficients of frequency-shift curve.

The experimental results illustrate the roving mass methodology for damage identification based only on structure damaged response. According to Rytter classification (Palechor, Bezerra, de Morais, *et al.*, 2019; Silva *et al.*, 2019), this method has level II, i.e., determine damage location but not damage quantification. The amplitudes of the wavelet coefficients can vary even if the same beam and damage are used in the same test since the signal processing is affected by the noise signal present, but the coefficients wavelets do not stop generating larger amplitudes in the regions proximate to the damage location.

## 5 Conclusions

This chapter presents applications of a non-destructive method called roving mass technique. This technique based on the frequencies shift using an additional roving mass presented coherent results for the two cases that were investigated (free-free and simply supported beam). This response-only technique, associated to Wavelet transforms, carry out damage localization in beam-like structures using numerical and experimental data. It was possible to locate the damage presence due to a discontinuity in modal frequency curve along beam. Also, it is possible to observe that the bigger the damage, the bigger this variation. The research works is developed at the Graduate Programs of Integrity of Engineering Materials and Structures and Civil Construction of University of Brasília.

Different mother wavelet functions (db5, coif3, sym6, and bior6.8) were analyzed with a better signal to noise ratio.

Finally, the proposed methodology has shown promise as it only needs to analyze the dynamic data of the damaged structure to successfully localize the damage, unlike other techniques that require the intact and damaged response.

## References

Aktan, A. E. *et al.* (1997) 'Structural Identification for Condition Assessment: Experimental Arts', *Journal of Structural Engineering*, 123(12), pp. 1674–1684. doi: 10.1061/(ASCE)0733-9445(1997)123:12(1674).

Breysse, D. *et al.* (2008) 'How to combine several non-destructive techniques for a better assessment of concrete structures', 38, pp. 783–793. doi: 10.1016/j.cemconres.2008.01.016.

Doebling, S. W. *et al.* (1996) *Damage identification and health monitoring of structural and mechanical systems from changes in their vibration characteristics.* California: Los Alamos National Laboratory.

Khoa, N. V. and Quang, N. Van (2016) 'Free vibration of a cracked double-beam carrying a concentrated mass', *Vietnam Journal of Mechanics*. Publishing House for Science and Technology, Vietnam Academy of Science and Technology (Publications), 38(4), pp. 279–293. doi: 10.15625/0866-7136/7118.

Kotambkar, M. S. (2014) 'Mass Loading Effect on Natural Frequency of Cracked Beam in Free-Free Condition', *International Journal of Engineering Research & Technology*. IJERT-International Journal of Engineering Research & Technology, 3(9). doi: 10.17577/IJERTV3IS090113.

Law, S. S. *et al.* (2005) 'Structural damage detection from wavelet packet sensitivity', *Engineering Structures*. Elsevier, 27(9), pp. 1339–1348. doi: 10.1016/J.ENGSTRUCT.2005.03.014.

Liu, Y., Li, Z. and Zhang, W. (2009) 'Crack detection of fibre reinforced composite beams based on continuous wavelet transform', *https://doi.org/10.1080/10589750902744992*. Taylor & Francis Group , 25(1), pp. 25–44. doi: 10.1080/10589750902744992.

Mermetas, V. and Erol, H. (2001) 'Effect of Mass Attachment on the Free Vibration', in *Proceedings of 8th International Congress on Sound and Vibration (ICSV 2001)*, pp. 2803–2810.

Mikami, S., Beskhyroun, S. and Oshima, T. (2009) 'Wavelet packet based damage detection in beam-like structures without baseline modal parameters', *http://dx.doi.org/10.1080/15732470802334795*. Taylor & Francis , 7(3), pp. 211–227. doi: 10.1080/15732470802334795.

National Instruments (2009) *The Fundamentals of FFT-Based Signal Analysis and Measurement in LabVIEW and LabWindows/CVI - National Instruments*.

Palechor, E. U. L. (2013) *Damage Identification in Steel Beams by Wavelets and Numerical/Experimental Signal (por. Identificação de Danos em Vigas Metálicas Utilizando Wavelets e Dados Numéricos e Experimentais)*. Universidade de Brasília. Available at: https://repositorio.unb.br/handle/10482/14814.

Palechor, E. U. L. *et al.* (2014) 'Damage Identification in Beams Using Experimental Data', *Key Engineering Materials*, 607, pp. 21–29. doi: 10.4028/www.scientific.net/KEM.607.21.

Palechor, E. U.L. *et al.* (2018) 'Dynamic Analysis of a Beam with Additional Auxiliary Mass Spatial Via Spectral Element Method', *Springer Proceedings in Mathematics and Statistics*. Springer New York LLC, 249, pp. 279–289. doi: 10.1007/978-3-319-96601-4_25/COVER/.

Palechor, Erwin Ulises Lopez *et al.* (2018) 'Identificação De Danos Em Vigas Metálicas Utilizando Massas Itinerantes Adicionais, Análise Experimental.', *Revista Sul-americana de Engenharia Estrutural*, 15(3). doi: 10.5335/rsaee.v15i3.7886.

Palechor, E. U. L., Bezerra, L. M., Morais, M. V. G. de, *et al.* (2019) 'Damage identification in beams using additional rove mass and wavelet transform', *Frattura ed Integrità Strutturale*, 13(49), pp. 614–629. doi: 10.3221/IGF-ESIS.49.56.

Palechor, E. U. L., Bezerra, L. M., de Morais, M. V., *et al.* (2019) 'Damage identification in beams using additional rove mass and wavelet transform', *Frattura ed Integrità Strutturale*, 13(49), pp. 614–629. doi: 10.3221/IGF-ESIS.49.56.

Palechor, E. U. L. *et al.* (2022) 'Fundamental Concepts on Wavelet Transforms', in.

Radzieński, M., Krawczuk, M. and Palacz, M. (2011) 'Improvement of damage detection methods based on experimental modal parameters', *Mechanical Systems and Signal Processing*, 25(6), pp. 2169–2190. doi: 10.1016/j.ymssp.2011.01.007.

Ren, W. X. and Sun, Z. S. (2008) 'Structural damage identification by using wavelet entropy', *Engineering Structures*. Elsevier, 30(10), pp. 2840–2849. doi: 10.1016/J.ENGSTRUCT.2008.03.013.

Rizos, P. F., Aspragathos, N. and Dimarogonas, A. D. (1990) 'Identification of crack location and magnitude in a cantilever beam from the vibration modes', *Journal of Sound and Vibration*. Academic Press, 138(3), pp. 381–388. doi: 10.1016/0022-460X(90)90593-O.

Santos, J. C. *et al.* (2019) 'FREQUENCY-BASED DAMAGE DETECTION IN BEAMS USING AN ADDITIONAL ROVING MASS', in UFU (ed.) *Proceedings of the 25th International Congress of Mechanical Engineering*. Uberlândia: ABCM. doi: 10.26678/ABCM.COBEM2019.COB2019-1103.

Santos, J. C. (2020) *Detecção de danos em vigas Timoshenko utilizando técnicas de variação de frequência por wavelet*. University of Brasilia. Available at: https://repositorio.unb.br/handle/10482/39090.

Schabowicz, K. (2010) 'State-of-the-art non-destructive methods for diagnostic testing of building structures – anticipated development trends', X(3), pp. 8–9. doi: 10.1016/S1644-9665(12)60133-2.

Silva, R. S. Y. R. C. *et al.* (2019) 'Damage detection in a reinforced concrete bridge applying wavelet transform in experimental and numerical data', *Frattura ed Integrità Strutturale*, 13(48), pp. 693–705. doi: 10.3221/IGF-ESIS.48.65.

Ticona Melo, L. R. *et al.* (2016) 'Identification of Modal Parameters in a Scale Model for a Railway Bridge', *http://dx.doi.org/10.1142/S0219455415500595*. World Scientific Publishing Company , 16(9). doi: 10.1142/S0219455415500595.

Wang, Q. and Deng, X. (1999) 'Damage detection with spatial wavelets', *International Journal of Solids and Structures*. Pergamon, 36(23), pp. 3443–3468. doi: 10.1016/S0020-7683(98)00152-8.

Zhong, S. and Oyadiji, S. O. (2008) 'Identification of cracks in beams with auxiliary mass spatial probing by stationary wavelet transform', *Journal of Vibration and Acoustics, Transactions of the ASME*. doi: 10.1115/1.2891242.

Zhong, S., Oyadiji, S. O. and Ding, K. (2008) 'Response-only method for damage detection of beam-like structures using high accuracy frequencies with auxiliary mass spatial probing', *Journal of Sound and Vibration*, 311(3–5), pp. 1075–1099. doi: 10.1016/j.jsv.2007.10.004.